Applied Surface Science 471 (2019) 516–520

Contents lists available at ScienceDirect

Applied Surface Science

journal homepage: www.elsevier.com/locate/apsusc

Full Length Article

Maskless formation of uniform subwavelength periodic surface structures by double temporally-delayed femtosecond laser beams

Sohail A. Jalil[a,b,c], Jianjun Yang[a], Mohamed ElKabbash[c], Subhash C. Singh[a,c], Chunlei Guo[a,c,*]

[a] State Key Laboratory of Applied Optics, Changchun Institute of Optics, Fine Mechanics and Physics, Chinese Academy of Sciences, Changchun 130033, China
[b] University of Chinese Academy of Sciences, Beijing 100049, China
[c] The Institute of Optics, University of Rochester, Rochester, NY 14627, USA

ARTICLE INFO

Keywords:
Laser-matter interaction
Nanostructures
FLIPSSs
Ultrafast phenomenon
Surface plasmon
Nanofabrication

ABSTRACT

Surface structures with nanoscale size and periodicity are important in controlling the flow of light as well as light-matter interaction. Fabrication of these periodic nanostructure requires sophisticated and expensive nanofabrication methods that limits large scale production of such structures. Laser induced periodic surface structures (LIPSS) is a scalable and cheap method to create periodic structures. However, they suffer from lacking a long-range order. Here, we present a maskless fabrication technique of creating highly uniform subwavelength structures on nickel surface, using two collinear femtosecond laser beams at various temporal delays. Our femtosecond laser induced periodic surface structures (FLIPSSs) show a high spatial uniformity with a grating period ranging between 320–350 nm. The high spatial uniformity is a consequence of using two pulsed beams with short inter-beam delay time due to reduction in the propagation length of excited surface plasmon polaritons (SPPs). The subwavelength period is due to grating splitting mechanism where the two beams sequentially interact with existing structures to create a superimposed grating. The demonstrated fabrication method enables large scale fabrication of regular sub-wavelength structures.

1. Introduction

Controlling light with nanoscale surface modifications is the cornerstone of modern nanophotonics that paves the way for a new generation of ultra-compact, integrated photonic devices with broad applications ranging from basic research to industrial applications [1–4]. Uniform nanostructures are mainly fabricated on planar substrates by top-down techniques, e.g., electron-beam lithography or focused-ion beam milling [5–8]. However, these techniques have low throughput, require multi-step fabrication processes, and are costly [9]. On the other hand, LIPSS [10,11] offer a high throughput and comparably low-cost alternative to fabricating periodic nanostructures. FLIPSSs create a grating-like structure with a period on the order of the incident light wavelength [4,12,13]. In general, FLIPSSs suffer from two major drawbacks. The lack of long-range uniformity in the periodic structures, i.e., the period and orientation of the formed structures, significantly reduces the surface structure quality and limits its practical applications [14,15]. This uniformity problem stems from the nature of FLIPSSs formation. Because FLIPSSs form due to the interference between the scattered light, or surface waves [16–18], from random roughness and the incident field, the formed structures have some randomness in their overall orientation. Another challenge is that the period of the formed structures is only slightly shorter than the incident wavelength [13,16]. Thus, creating subwavelength structures essentially remains challenging.

One approach to address the FLIPSSs quality problem is by using positive and negative feedback mechanisms on titanium substrates [19]. However, the feedback mechanism is not universal as it requires using non-noble metals that can form oxides easily. Furthermore, it was shown that [20], uniform FLIPSS are formed on metals with short surface plasmon polariton (SPP) propagation length, as we will discuss in detail later. Finally, uniform FLIPSS on dielectrics and semiconductors were produced by exciting SPPs at the dielectric-plasma interface [21]. On the other hand, sub-wavelength line gratings were realized by splitting FLIPSSs grating either by varying the laser beam dose during line scanning [22], or via localizing the electromagnetic field on the protuberance of already existing FLIPSSs [23]. However, the subwavelength gratings produced by the grating splitting method, so far, also lack uniformity and are of low quality.

In this work, we report the formation of uniform FLIPSSs with

* Corresponding author at: The Institute of Optics, University of Rochester, Rochester, NY 14627, USA.
E-mail address: guo@optics.rochester.edu (C. Guo).
URL: http://www2.optics.rochester.edu/workgroups/guo/index.html (C. Guo).

https://doi.org/10.1016/j.apsusc.2018.12.029
Received 15 October 2018; Received in revised form 1 December 2018; Accepted 4 December 2018
Available online 05 December 2018
0169-4332/

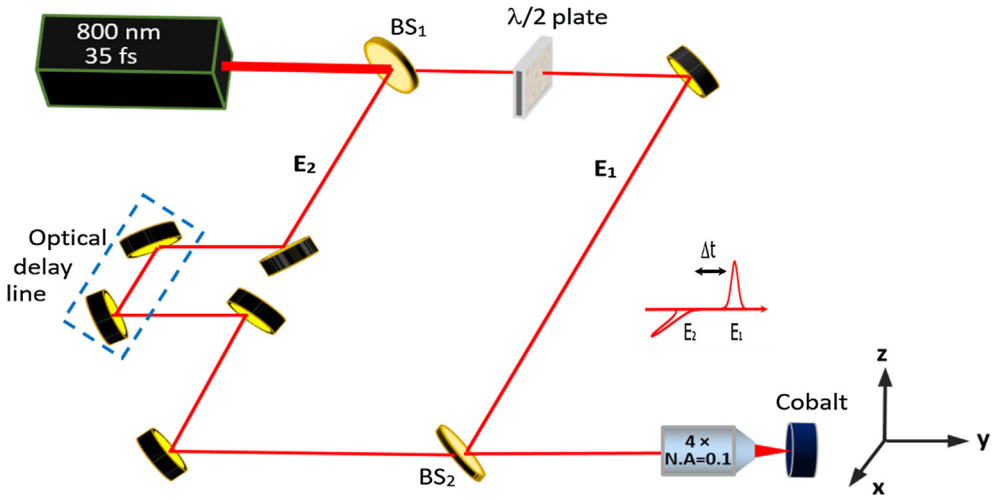

Fig. 1. Experimental setup for the formation of high uniformity 1D FLIPSS structures using two temporally delayed femtosecond laser beams.

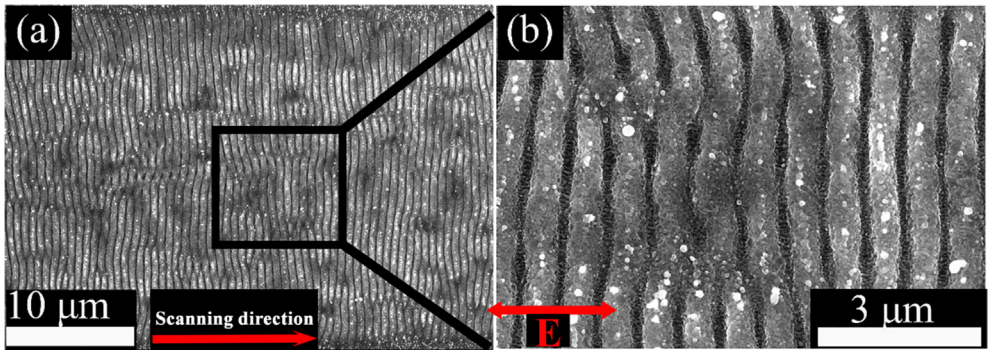

Fig. 2. SEM images of the FLIPSSs formation at the optimal fluence (F = 0.22J/cm^2), scanning speed (v = 0.3 mm/sec) and distance from the focal point (300 μm) single beam (a). (b) The magnified view of the marked region in (a).

subwavelength period on nickel using two collinearly propagated and temporally delayed beams of laser pulses with different polarizations. The uniformity originates from using two beams as we demonstrate by comparing the uniformity of FLIPSSs produced by single and two laser beams. In addition, we demonstrate a grating splitting that occurs only for the two laser beams configuration. Consequently, using two spatially overlapping yet temporally-delayed beams we realize subwavelength periodicity with high quality. We propose the possible mechanisms behind the uniformity and subwavelength periodicity that are unique to using two delayed femtosecond laser beams.

2. Experimental methods

A diagram of the experimental setup is shown in Fig. 1, where a Ti: sapphire femtosecond laser amplifier (Spectra Physics HP-Spitfire) was used as an irradiation source to deliver horizontally polarized pulse trains at a repetition rate of 1kHz, with a central wavelength of λ = 800 nm and time duration of τ = 35fs. To study the effect of ultrafast surface dynamics on the microstructure formation, a Mach-Zehnder interferometer was introduced, which split each output pulse from the laser amplifier into two parts with equal energy by a beam splitter, BS_1. A half wave plate ($\lambda/2$) was inserted in one of the optical paths to rotate the light polarization, thus making the two beams to possess 30Â° between their linear polarizations. The arrival time of the two laser beams onto the target surface was adjusted by changing the optical delay line within one of the beam paths. After spatially overlapping together by another beam splitter, BS_2, the two laser beams were focused through an objective lens (4 × ,N. A = 0.1) at normal incidence. A bulk Ni plate (with 10 mm in diameter and 2 mm in thickness) was mounted on a three-dimensional precision translation stage. Ni was chosen due to its attractive properties, e.g., high curie temperature and superior magneto-restrictive properties with many potential applications such as a cathode for water purification and field emission enhancement [24,25]. The surface structuring was performed in a scanning mode with a constant speed of 0.30mm/s, leading to 172 laser pulses partially overlapped within one laser spot area. After the laser structuring process, the surface morphological features were analyzed by scanning electron microscopy (SEM).

3. Results and discussion

To determine the effect of using double pulse femtosecond laser in realizing uniform FLIPSSs, we first investigate the uniformity of single pulsed FLIPSSs at various fabrication parameters. We varied the fluence (F = 0.1 − 0.4J/cm^2), scanning speed (v = 0.01–1 mm/sec), and distance from the focal point (0–600 μm). The optimal results are presented in Fig. 2a and b and was obtained using F = 0.22J/cm^2, v = 0.3 mm/sec, and 300 μm distance from the focal point. As shown in Fig. 2a and b, a well-defined FLIPSSs structures observed with periodicity $\Lambda^{\text{Single beam}}$ 660 nm. The grooves orientation is perpendicular to the incident laser polarization (horizontal direction as marked by E in Fig. 2(b)). The FLIPSSs, however, are of low spatial-uniformity as they have a wavy-like spatial distribution, i.e., the alignment of each groove is twisted into many bends rather than a straight line. In our case, the formation of FLIPSSs is attributed to the laser-surface plasmons (SPs) interference as illustrated in [13,16]. The non-uniform, low quality, line gratings are frequently reported in previous works using fixed shot or scanning of single beam [4,13,16]. This is due to the random scattering

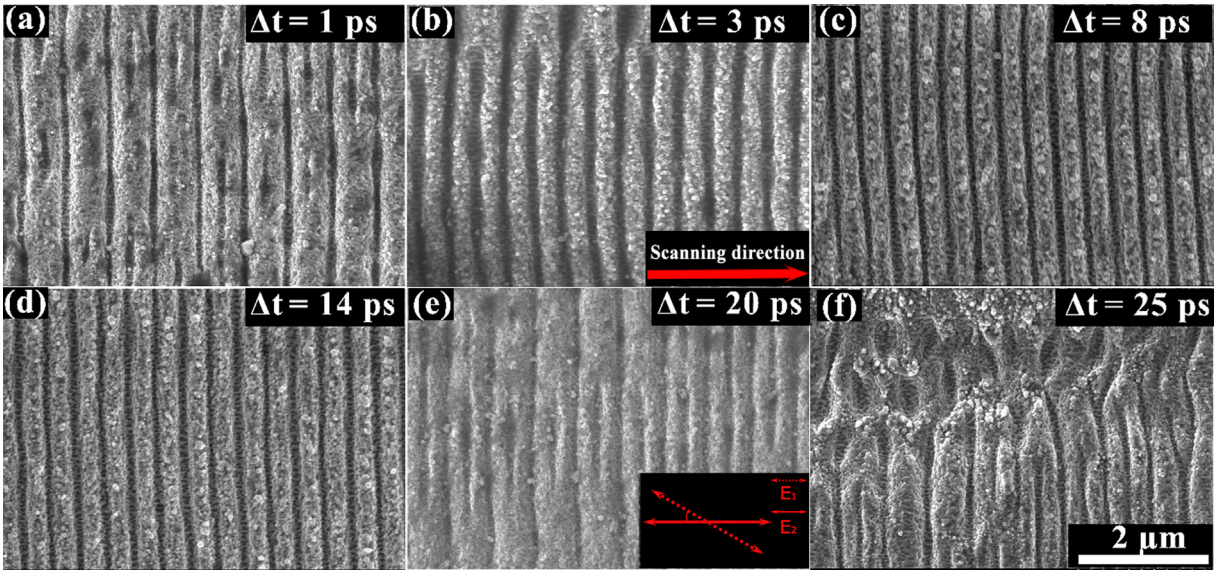

Fig. 3. SEM images of the FLIPSSs formation using two time-delayed beams at a total fluence of 0.22J/cm^2, and time delays of 1ps < Δτ < 25ps. The red double headed arrows show the polarization intersection angle of 30Â° between two laser beams. The red arrow shows the scanning direction of the target. The scale bar is 2 μm for Fig. 3(a–f).

sources that act as seed points for FLIPSSs [16,26]. At the highest fluence of F = 0.30J/cm^2, excessive melting was observed; thus, we choose F = 0.22J/cm^2, throughout the surface structuring.

We then used double collinear beams with different polarizations such that the pulses arrive with a controlled inter-pulse delay Δτ. The polarization intersection angle between two beams is 30Â°. Note that it is necessary to use different polarizations otherwise the system interacts with the two beams as a single, delayed, beam. The laser fluence of each beam is 0.11J/cm^2 which is below the threshold necessary to create uniform FLIPSSs, however, the net energy fluence of both beams is equal to the fluence required to create structures on the entire scanned line as shown in Fig. 2 (0.22J/cm^2) which is above the FLIPSSs threshold. We varied Δτ from 1 ps to 26 ps and investigated the properties of the formed FLIPSSs as a function of delay time. Two interesting features are observed; (i) the generated FLIPSSs is significantly more uniform, (ii) the grating peaks split over time and complete grating splitting is observed within Δτ = 6 ps to 14 ps. Accordingly, the FLIPSSs period reduces by half to $\Lambda^{\text{Double pulsed beam}}$ 350 nm. For Δτ > 14 ps, the grating splitting progressively recedes and at Δτ = 25 ps the gratings lose uniformity. Finally, we note that spatial orientation of FLIPSSs is always perpendicular to the polarization direction of the second laser beam due to laser-SPs interference as was previously reported [27].

A quantitative description of the above-mentioned grating splitting processes as a function of the time delay Δτ. is shown in Fig. 4. The inset of Fig. 4 shows an image of SEM marked with different lines for the clear understanding of the terms; grating splitting, grooves width and FLIPSSs periodicity. We measured the grating splitting, grooves width and FLIPSSs periodicity for the uniform time range where the grating splitting is evident (Δτ = 6–14 ps). Each data point corresponds to the average of four different points and the error is estimated as the standard deviation. Two different types of grooves are formed i.e., smaller one, (marked with black lines in Fig. 4), due to grating splitting (maximum width of 90 nm), and larger one (marked with red lines in Fig. 4), results from FLIPSSs formation (maximum width of 123 nm). The grating splitting, grooves and FLIPSSs periodicity is respectively marked with black, red and blue lines where the slight increasing trend in periodicities with the increase in time delay (from Δτ = 6 − 14 ps) for all cases can be seen. The periodicity of these FLIPSSs ranges from 320 − 350 nm, with a constant ridge width of 220 nm.

The creation of the FLIPSSs orthogonal to the second beams polarization is further proven by rotating the polarization of both beams

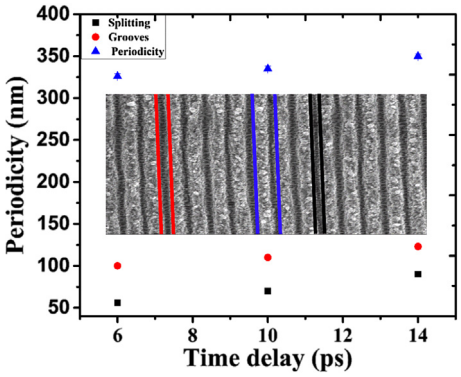

Fig. 4. Measured FLIPSSs period, groove width and grating splitting are marked by blue, red and black lines, respectively. The graph shows the increasing trend of these parameters as a function of time-delay. Each data point corresponds to the average of four different points and the error is estimated as the standard deviation.

while maintaining the polarization intersection angle as 30Â° and a time delay of Δτ = 6 ps as shown in Fig. 5. This demonstration shows that the FLIPSSs orientation is entirely due to the second beam. However, since the second pulsed beam energy is below the FLIPSSs threshold, the first pulsed beam must play an essential role in creating the uniform FLIPSSs and the observed grating splitting. Clearly, the grooves and ridges are very uniform even without grating splitting which indicates that they do not share the same physical origin.

The uniformity of the double pulse FLIPSSs is likely due to the modification of the propagation length of SPPs excited by the second pulse, due to altering the material's optical properties by the first pulse [28,29]. SPPs are electromagnetic surface waves taking the form of propagating charge oscillations at a metal-dielectric interface [30]. The propagation length of SPPs is $L_{SPP} = 1/2\beta''$, where β'' is the imaginary component of the complex SPP wavenumber [20]. It has been shown recently [20], that FLIPSSs uniformity is governed by the decay length of SPPs; shorter L_{SPP} provide more uniform FLIPSSs. This conclusion is rational as shorter L_{SPP} implies less interaction of the excited surface wave with surface irregularities. In the double pulse case, the first pulse clearly modifies the transient complex refractive index ($n = n' + in''$) [31], where n' and in'' are the real and imaginary parts of refractive

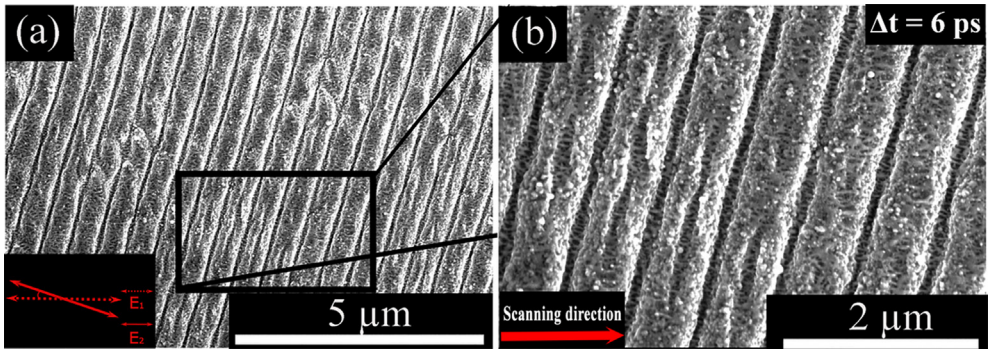

Fig. 5. FLIPSSs structures at different polarization direction of incident first and second beam or at the negative delay time. The red double headed arrows show the polarization intersection angle of 30Â° between two laser beams.

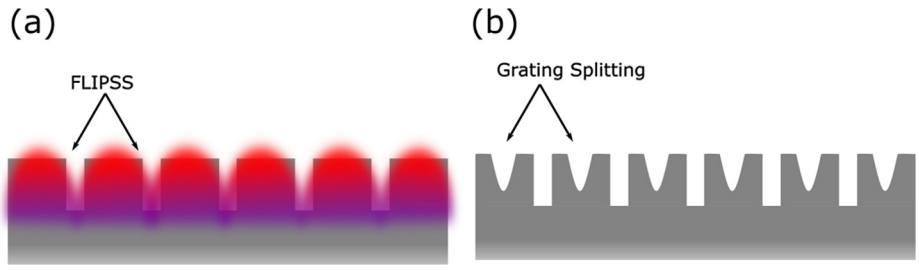

Fig. 6. Proposed mechanisms behind the observed grating splitting effect: (a) Following the formation of uniform FLIPSSs, the field variation across the grooves leads to higher field intensity in the protuberance which accumulates enough energy to allow formation of superimposed FLIPSSs. (b) The latter start forming on the protuberance resulting in splitting the gratings.

index. Of the metallic substrate. In particular, the reflectance R and L_{SPP} has certainly changed, where $\delta L_{SPP}/\delta n'$ and $\delta L_{SPP}/\delta n''$ have the same sign as $\delta R/\delta n'$ and $\delta R/\delta n''$, respectively, as long as $n'' > n$, which is true for all metals including Ni [30]. Since the transient differential reflection ($\Delta R/R$) of Ni excited at 800 nm is negative, i.e., δR is negative, as shown in Ref. [32], we can conclude that the modification in n leads to a shorter L_{SPP}, hence, more uniform LIPSS. We note here, that in the case of a single pulse, the temporal evolution of L_{SPP} was studied and showed that over the pulse duration, L_{SPP} also decreases over time [20].

Fig. 6 shows the proposed mechanisms behind the observed grating splitting mechanism. After the formation of uniform FLIPSSs, the well-known positive feedback mechanism due to the interaction between the incident radiation and the existing structure further deepens the grooves [23,26]. As evident from Figs. 3 and 5, the grating splitting mechanism occurs after the formation of FLIPSSs with period $\Lambda^{\text{Single beam}}$. When the grooves are deep enough, the field intensity of irradiated light will vary significantly between the grooves and the protuberance [23] as shown schematically in Fig. 6a. Because each beam has intensity lower than the FLIPSSs threshold, only regions where the two beams deposits enough energy can subsequently form FLIPSSs. Since the grooves are created where the maximum field intensity exist, superimposed FLIPSSs starts to form on top of the existing FLIPSSs, where a positive feedback mechanism results in deepening the grooves further which splits the grating (Fig. 6b).

4. Conclusion

In this work, we demonstrated a single-step method to rapidly fabricate uniform and subwavelength 1D FLIPSSs structures using two temporally delayed, collinear beams with linear polarization intersection angle of 30Â°. We show that the FLIPSSs structures formed are orthogonal to the second delayed beam. Compared with the irregular 1D grating-like FLIPSSs structures induced by single femtosecond laser beam, highly uniform 1D FLIPSSs have been produced by employing two time-delayed laser beams. The uniformity is likely due to the shortening of the SPP propagation length L_{SPP} following the modification of the metal optical properties due to the first pulse. Moreover, the FLIPSSs undergoes a grating splitting phenomenon that leads to short period FLIPSSs. Our experiments suggest that the variation of field intensity across already existing FLIPSSs is responsible for the grating splitting phenomenon. Our investigations can provide deep insights into femtosecond laser processing of materials using two delayed beams and can be a starting point for realizing a universal method for fabricating subwavelength uniform nanostructures.

Acknowledgements

This work is financially supported by the National Key R&D Program of China (2017YFB1104700), National Natural Science Foundation of China (11674178), Jilin Provincial Science & Technology Development Project (20180414019GH), Tianjin National Natural Science Foundation (12JCZDJC20200), and Bill & Melinda Gates Foundation (OPP1119542).

References

[1] L. Feng, S. Li, Y. Li, H. Li, L. Zhang, J. Zhai, Y. Song, B. Liu, L. Jiang, D. Zhu, Super-hydrophobic surfaces: from natural to artificial, Adv. Mater. 14 (2002) 1857–1860, https://doi.org/10.1002/adma.200290020.
[2] Y. Xia, P. Yang, Y. Sun, Y. Wu, B. Mayers, B. Gates, Y. Yin, F. Kim, H. Yan, One-dimensional nanostructures: synthesis, characterization, and applications, Adv. Mater. 15 (2003) 353–389, https://doi.org/10.1002/adma.200390087.
[3] K. Sugioka, Y. Cheng, Ultrafast lasers—reliable tools for advanced materials processing, Light Sci. Appl. 3 (2014) e149, https://doi.org/10.1038/lsa.2014.30.
[4] J. Bonse, S. Höhm, S.V. Kirner, A. Rosenfeld, J. Krüger, Laser-induced periodic surface structures—a scientific evergreen, IEEE J. Sel. Top. Quant. Electron. 23 (2017) 109–123, https://doi.org/10.1109/JSTQE.2016.2614183.
[5] T. Ito, S. Okazaki, Pushing the limits of lithography, Nature 406 (2000) 1027, https://doi.org/10.1038/35023233.
[6] G.M. Whitesides, B. Grzybowski, Self-assembly at all scales, Science 295 (2002) 2418–2421, https://doi.org/10.1126/science.1070821.
[7] F. Watt, A. Bettiol, J. Van Kan, E. Teo, M. Breese, Ion beam lithography and nanofabrication: a review, Int. J. Nanosci. 4 (2005) 269–286, https://doi.org/10.1142/S0219581X05003139.
[8] M. Altissimo, E-beam lithography for micro-/nanofabrication, Biomicrofluidics 4 (2010) 026503, https://doi.org/10.1063/1.3437589.
[9] A.A. Tseng, K. Chen, C.D. Chen, K.J. Ma, Electron beam lithography in nanoscale fabrication: recent development, IEEE Trans. Electronic. Packag. Manuf. 26 (2003) 141–149, https://doi.org/10.1109/TEPM.2003.817714.
[10] M. Birnbaum, Semiconductor surface damage produced by ruby lasers, J. Appl. Phys. 36 (1965) 3688–3689, https://doi.org/10.1063/1.1703071.
[11] J. Sipe, J.F. Young, J. Preston, H. Van Driel, Laser-induced periodic surface structure. I. Theory, Phys. Rev. B 27 (1983) 1141, https://doi.org/10.1103/PhysRevB.

27.1141.
[12] A.Y. Vorobyev, C. Guo, Femtosecond laser-induced periodic surface structure formation on tungsten, J. Appl. Phys. 104 (2008) 063523, https://doi.org/10.1063/1.2981072.
[13] A.Y. Vorobyev, C. Guo, Direct femtosecond laser surface nano/microstructuring and its applications, Laser Photon. Rev. 7 (2013) 385–407, https://doi.org/10.1002/lpor.201200017.
[14] A. Borowiec, H. Haugen, Subwavelength ripple formation on the surfaces of compound semiconductors irradiated with femtosecond laser pulses, Appl. Phys. Lett. 82 (2003) 4462–4464, https://doi.org/10.1063/1.1586457.
[15] F. Costache, S. Kouteva-Arguirova, J. Reif, Sub–damage–threshold femtosecond laser ablation from crystalline Si: surface nanostructures and phase transformation, Appl. Phys. A 79 (2004) 1429–1432, https://doi.org/10.1007/s00339-004-2803-y.
[16] A.Y. Vorobyev, V. Makin, C. Guo, Periodic ordering of random surface nanostructures induced by femtosecond laser pulses on metals, J. Appl. Phys. 101 (2007) 034903, https://doi.org/10.1063/1.2432288.
[17] T.Y. Hwang, A.Y. Vorobyev, C. Guo, Ultrafast dynamics of femtosecond laser-induced nanostructure formation on metals, Appl. Phys. Lett. 95 (2009) 123111, https://doi.org/10.1063/1.2146067.
[18] E. Gurevich, S. Gurevich, Laser induced periodic surface structures induced by surface plasmons coupled via roughness, Appl. Surf. Sci. 302 (2014) 118–123, https://doi.org/10.1016/j.apsusc.2013.10.141.
[19] B. Öktem, I. Pavlov, S. Ilday, H. Kalaycıoğlu, A. Rybak, S. Yavaş, M. Erdoğan, F.Ö. Ilday, Nonlinear laser lithography for indefinitely large-area nanostructuring with femtosecond pulses, Nat. Photon. 7 (2013) 897, https://doi.org/10.1038/nphoton.2013.272.
[20] I. Gnilitskyi, T.J.-Y. Derrien, Y. Levy, N.M. Bulgakova, T. Mocek, L. Orazi, High-speed manufacturing of highly regular femtosecond laser-induced periodic surface structures: physical origin of regularity, Sci. Rep. 7 (2017) 8485, https://doi.org/10.1038/s41598-017-08788-z.
[21] L. Wang, Q.-D. Chen, X.-W. Cao, R. Buividas, X. Wang, S. Juodkazis, H.-B. Sun, Plasmonic nano-printing: large-area nanoscale energy deposition for efficient surface texturing, Light Sci. Appl. 6 (2017) e17112, https://doi.org/10.1038/lsa.2017.112.
[22] P. Feng, L. Jiang, X. Li, K. Zhang, X. Shi, B. Li, Y. Lu, Femtosecond laser-induced subwavelength ripples formed by asymmetrical grating splitting, Appl. Surf. Sci. 372 (2016) 52–56, https://doi.org/10.1016/j.apsusc.2016.02.195.
[23] S. Hou, Y. Huo, P. Xiong, Y. Zhang, S. Zhang, T. Jia, Z. Sun, J. Qiu, Z. Xu, Formation of long-and short-periodic nanoripples on stainless steel irradiated by femtosecond laser pulses, J. Phys. D 44 (2011) 505401, https://doi.org/10.1088/0022-3727/44/50/505401.
[24] S.A. Jalil, S. Bashir, M. Akram, Q. Ahmed, F. Haq, Surface morphology correlated with field emission properties of laser irradiated nickel, Indian J. Phys. 91 (2017) 953–965, https://doi.org/10.1007/s12648-017-0979-1.
[25] Y. Zhu, T. Liu, L. Li, S. Song, R. Ding, Nickel-based electrodes as catalysts for hydrogen evolution reaction in alkaline media, Ionics 24 (2018) 1121–1127, https://doi.org/10.1007/s11581-017-2270-z.
[26] M. Huang, F. Zhao, Y. Cheng, N. Xu, Z. Xu, Origin of laser-induced near-subwavelength ripples: interference between surface plasmons and incident laser, ACS Nano 3 (2009) 4062–4070, https://doi.org/10.1021/nn900654v.
[27] S. Höhm, M. Herzlieb, A. Rosenfeld, J. Krüger, J. Bonse, Dynamics of the formation of laser-induced periodic surface structures (LIPSS) upon femtosecond two-color double-pulse irradiation of metals, semiconductors, and dielectrics, Appl. Surf. Sci. 374 (2016) 331–338, https://doi.org/10.1016/j.apsusc.2015.12.129.
[28] T. Donnelly, J. Lunney, S. Amoruso, R. Bruzzese, X. Wang, X. Ni, Double pulse ultrafast laser ablation of nickel in vacuum, J. Appl. Phys. 106 (2009) 013304, https://doi.org/10.1063/1.3159010.
[29] Z. Hu, S. Singha, Y. Liu, R.J. Gordon, Mechanism for the ablation of Si〈111〉 with pairs of ultrashort laser pulses, Appl. Phys. Lett. 90 (2007) 131910, https://doi.org/10.1063/1.2716838.
[30] K.F. MacDonald, Z.L. Sámson, M.I. Stockman, N.I. Zheludev, Ultrafast active plasmonics, Nat. Photon. 3 (2009) 55, https://doi.org/10.1038/nphoton.2008.249.
[31] M. ElKabbash, A.R. Rashed, B. Kucukoz, Q. Nguyen, A. Karatay, G. Yaglioglu, E. Ozbay, H. Caglayan, G. Strangi, Ultrafast transient optical loss dynamics in exciton–plasmon nano-assemblies, Nanoscale 9 (2017) 6558–6566, https://doi.org/10.1039/C7NR01512G.
[32] P.E. Hopkins, J.M. Klopf, P.M. Norris, Influence of interband transitions on electron-phonon coupling measurements in Ni films, Appl. Opt. 46 (2007) 2076–2083, https://doi.org/10.1364/AO.46.002076.